



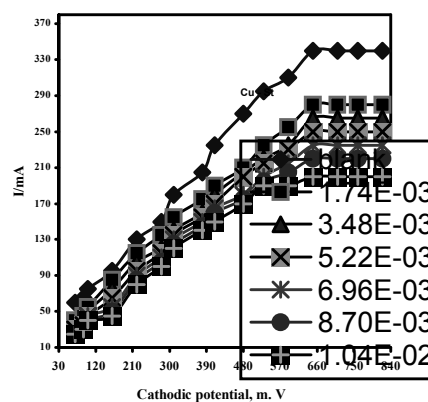
## ELECTRODEPOSITION USING ROTATING CYLINDER ELECTRODE OF COPPER IN PRESENCE OF ORGANIC COMPOUNDS

Mervette EL BATOUTI and Abdel-Moneim M. AHMED

Chemistry Department, Faculty of Science, Alexandria University, Egypt

Received July 28, 2016

This study shows the effect of using different organic compounds as accelerators for copper electrodeposition. High deposition rate is attributed to the enhanced mass transport of copper ions toward the metal surface and lowering the viscosity through the acidic bath using the rotating cylinder technique. The effect of different concentrations of organic compounds in the process of electrodeposition of copper from acidified copper sulfate solutions, has been studied at different temperatures, a node type, different rotation speeds, and additive concentration due to the changes in the physicochemical properties of the mixture. Overall mass transfer correlations have been obtained using the dimensional analysis method. The results agreed with the previous studies of mass transfer to rotating cylinders in turbulent flow systems.



Effect of acetic acid on limiting current in a mixture of 1.5 M H<sub>2</sub>SO<sub>4</sub>, 0.15 M copper sulphate and different concentrations (mol/l).

### INTRODUCTION

The rotating cylinder electrochemical reactor (RCE) is one of the most common geometries for different types of studies, such as metal ion recovery,<sup>1-3</sup> alloy formation,<sup>1,2</sup> corrosion,<sup>1,2</sup> effluent treatment<sup>4-8</sup> and Hull cell studies.<sup>9,10</sup> RCEs are also particularly well suited for high mass transport studies in the turbulent flow regime.<sup>2,11-14</sup> In practical operating conditions, the electrochemical reaction is directly related to the reactor hydrodynamics.<sup>15</sup> While considering the above, it is important to emphasize that hydrodynamic studies in these cells are rather limited. The flow pattern in the rotating cylinder cell has been approximated in turbulent flow.<sup>16,17</sup> The theoretical

approximation of this pattern has been developed by using the ensemble-averaged Navier-Stokes equation to model turbulent flow around a rotating cylinder, coupling boundary condition of the Dirichlet and Newman.<sup>16</sup> In addition, these authors<sup>16</sup> showed that in the fully turbulent layer, a logarithmic velocity profile exists, which is similar to that developed inside tubes and over flat plates.<sup>17</sup> Another approximation employs the Reynolds Averaged Navier-Stokes (RANS) equations, which include the turbulent viscosity by means of k-ε turbulent model.<sup>18,19</sup> One of the difficulties of using turbulence models is the presence of solid walls, since turbulence models are not applicable in the proximity of the wall.<sup>17</sup> Rivero *et al.*<sup>18</sup> solved this problem coupling the

\* Corresponding author: mervette\_b@yahoo.com

universal logarithmic wall functions to the rotating and outer boundaries. These authors employed a laboratory scale RCE, with the singularity of the counter electrode in a hexagonal array. The theoretical results showed the presence of Taylor vortices around the cylinder surface,<sup>19</sup> which were not observed in the work performed by Hwang and coworkers.<sup>17,18</sup> Tzayam Pérez, José L. Nava studied experimentally the influence of using a four-plate, six-plate and concentric cylinder as counter electrodes on mass transport.<sup>15,16</sup> In that research, we found that the counter electrode arrangement has an important role in the hydrodynamic behavior, emphasizing that the four-plate device gives greater turbulence-promoting action on the RCE interface than the others. The above findings are important from a technical and economic standpoint in the design of this type of electrochemical cell. However, theoretical hydrodynamic studies are rather limited.

Metals deposited in a very rough or powder form, when the electrolysis carried out at limiting current. This seems to be a rather general rule<sup>20</sup> in the case of copper. The possibility preventing powder formation at the limiting current by means of suitable additives is of interest electroplating<sup>21</sup> and electrometallurgy in general. Some organic substances used as additives in electroplating, electrowinning and electroforming to improve the quality of electrodeposits, since they produce fine-grained smooth bright deposit. Although the exact mechanism by which the organic compound added improves the quality of the electrodeposits is not known, there is a consensus that adsorption of those substances on the metal is involved, where adsorption of these organic compounds on the cathode surface may block a part of the active electrode area and therefore reduce the limiting current.

The objective of the present work is to show the effects of concentric cylinder when used as the counter electrodes on the turbulent flow of a rotating cylinder electrode. It is also to investigate copper electrodeposition from acidified solutions of copper sulfate mixed with different contents of organic additives such as: Acetic acid (I), Formamide (II), Ethylamine (III), 2-Methoxy ethanol (IV), Glycine (V) and Acetonitrile (VI) under natural and forced convection. Such investigation included changes in temperature, concentration of organic additives, speed of rotating cylinder electrode (RCE), and a node type.

The influence of the structure of organic additives related inhibitors on the mechanism and kinetics of inhibition of electrodeposition process.

## EXPERIMENTAL

### Chemicals

Analar grade  $\text{CuSO}_4 \cdot 5\text{H}_2\text{O}$  and  $\text{H}_2\text{SO}_4$  (98% w/w), supplied by BDH Chemicals Ltd., were used for the preparation of the electrolytes. Sodium carbonate, acetic acid, potassium iodide and potassium thiosulphate supplied by BDH Chemical Ltd., were used to check the concentration of copper sulfate. Solutions were prepared with water of resistivity of 18 M.Ω.cm, which was obtained from a MilliRo / MilliQ water purification system. Analar grade Compound I Acetic acid, Compound II Formamide, Compound III Ethylamine, Compound IV 2-Methoxy ethanol, Compound V Glycine and Compound VI Acetonitrile supplied by BDH Chemicals Ltd., were used as organic additives.

### Method of solution preparation

All chemicals were Analar grade and supplied by BDH Chemicals Ltd. The concentration of organic compounds was varied from  $1.74 \times 10^{-3}$ – $10.04 \times 10^{-3}$  mol/L. The sulphate and sulphuric acid (98%)w/w concentration were 0.15M respectively. For all experiments, copper sulphate concentration was checked Iodometry. The total volume of the electrolytic bath solution was made up to 300ml. Double distilled water with measured resistivity  $>18$  M.Ω.cm used in preparation of solutions.

### The Rotating Cylinder Electrode (RCE)

Fig. 1 shows that the voltmeter is connected in parallel to the cell to measure its voltage. The cathode consisted of Cu metal cylinder 1 cm diameter and 5 cm length. The disk is insulated by epoxy resin. The anode is made of cylindrical copper metal counter electrode of 12 cm diameter; it's also acted as the reference electrode by virtue of its high surface area compared to that of the cathode.

## RESULT AND DISCUSSION

### Effect of Concentration of $\text{CuSO}_4$ on the Limiting Current

The effect of copper sulfate concentration on the limiting current in Cu-St, is obvious that limiting current increases as copper sulfate increases.<sup>22</sup> Increasing the  $\text{CuSO}_4$  content in the bath, decreases the cathodic polarization and increases the limiting current plateau. These results were expected due to an increase in the relative abundance of the uncomplexed  $\text{Cu}^{2+}$  ions in the solution.<sup>23</sup>

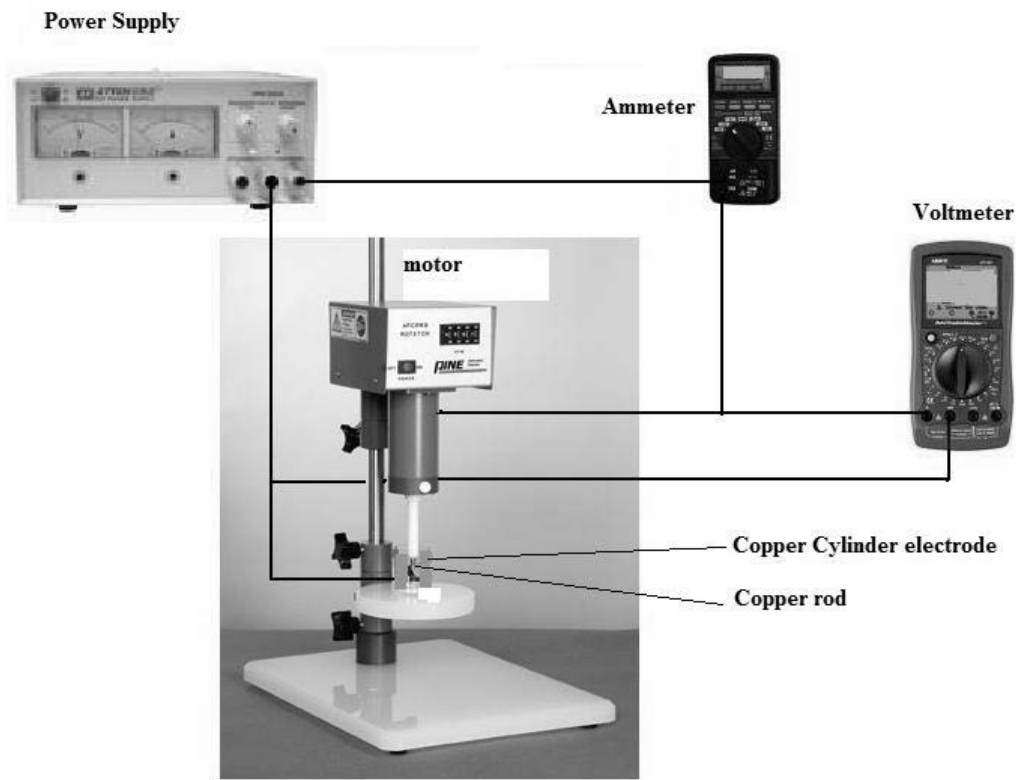


Fig. 1 – The rotating cylinder electrode electrolytic cell and the electrical circuit.

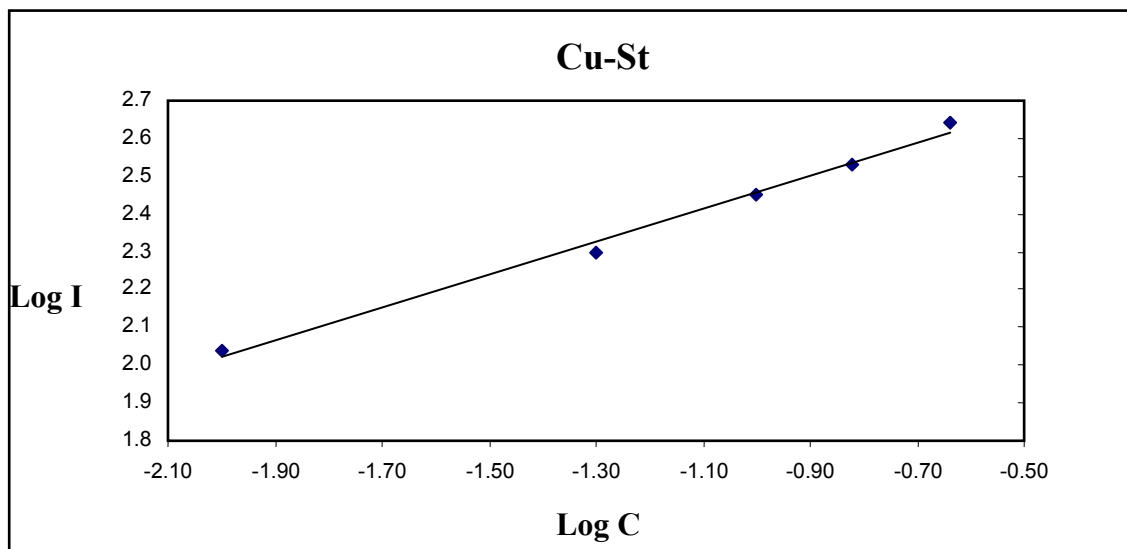
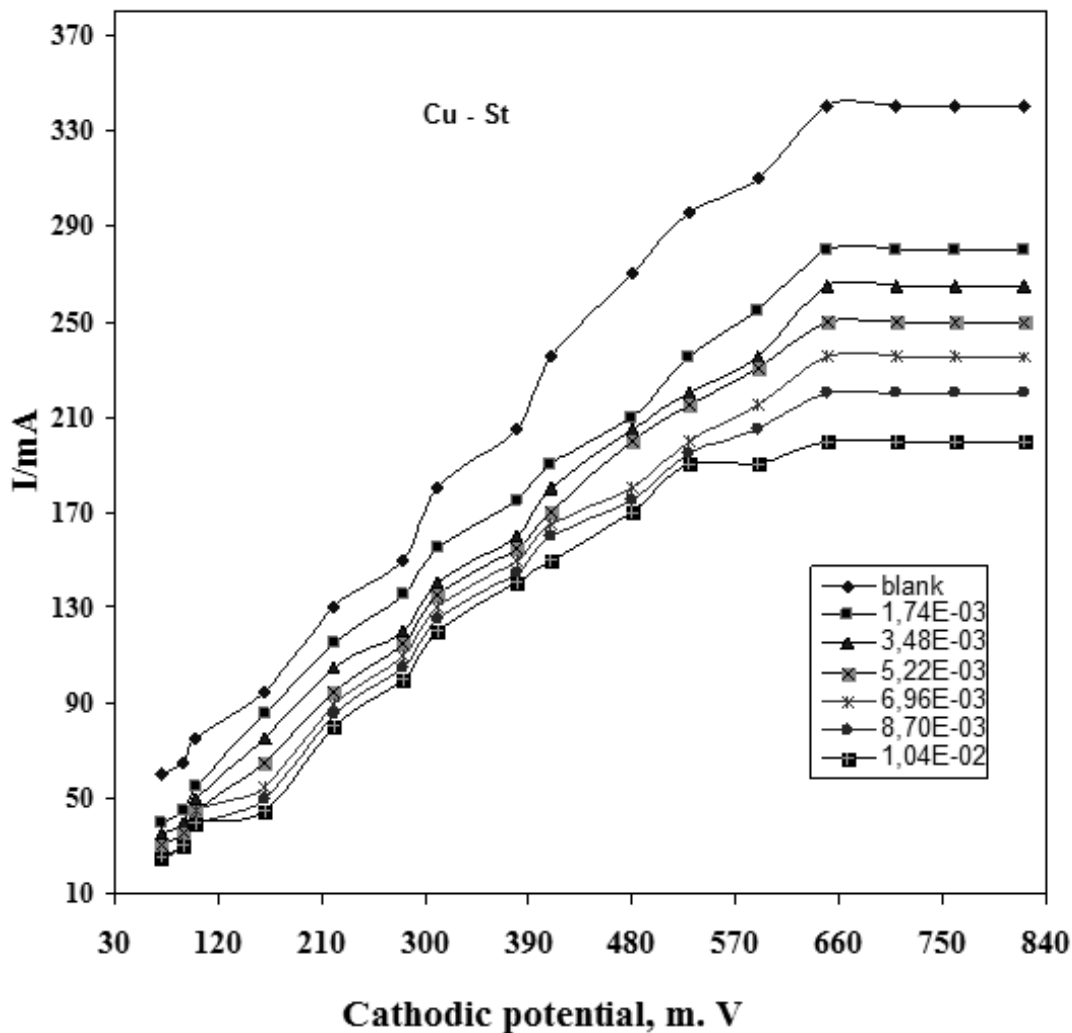


Fig. 2 – The relation between log I and log C in case of Cu-St at 298 K.

### Potentiodynamic Cathodic Polarization Curves

Tables 1 give the relation between current and volt at different conditions. Figs. 3 show the cathodic polarization curves for copper

electrodeposition from sulfate solution under the influence of adding different amounts of organic compound (I). It is obvious that in the organic, free solution, the current, first, increases linearly, then tend to exhibit limiting current plateau with increasing the cathodic potential.<sup>24</sup>



Effect of acetic acid on limiting current in a mixture of 1.5 M H<sub>2</sub>SO<sub>4</sub>, 0.15 M copper sulphate and different concentrations (mol/l).

Fig. 3 – Polarization Curve in case of (Cu-St) at 298 k for different concentrations of compound I.

The observed changes in the cathodic polarization in the presence of organic compound suggest that it must be acting as an inhibitor, which confirmed by the observation that at any given over-potential, the current density for copper deposition from solutions containing organic compound is lower than that found in the corresponding organic free solution. This inhibition of the organic compound in the copper electroplating reaction may be due to the adsorption of organic compound on the cathode surface. Therefore, the limiting current decreases with increasing organic concentration as shown in Figs. 3 due to a lowering of the complexes Cu<sup>2+</sup> ions. Values by limiting current for all solutions at different temperatures using copper anode and in

another case using stainless steel anode were given in Table (1). Noticeably, Table (1) shows that the limiting current decreases with increasing organic additives concentration and increases with temperature. The values of limiting current density I<sub>l</sub> for all solutions at different temperatures were used to calculate the mass transfer coefficient, K from the equation:<sup>25</sup>

$$K = i_l / zFA C_0 \quad (1)$$

where, z: number of electrons involved in the reaction, F: Faraday constant (A.s. mol<sup>-1</sup>), C<sub>0</sub>: bulk concentration of copper sulfate (mol/cm<sup>3</sup>), A: electrode area.

Table 1

Values by limiting current for all solution at different temperatures using stainless steel anodes

Organic additives	C mol/L	Limiting current (mA)			
		Stainless Steel anode			
		25° C	30° C	35° C	40° C
	Blank	340	370	405	440
Acetic acid	1.74E-03	280	300	325	350
	3.48E-03	265	285	310	335
	5.22E-03	250	270	290	310
	6.96E-03	235	255	275	295
	8.70E-03	220	235	255	275
	1.04E-02	200	215	230	245
Formamide	2.95E-03	330	355	380	410
	5.90E-03	310	330	360	390
	8.85E-03	290	315	340	360
	1.18E-02	275	295	320	340
	1.48E-02	260	275	295	315
	1.77E-02	240	255	275	290
Ethylamine	1.53E-03	250	275	300	325
	3.04E-03	240	265	290	305
	4.56E-03	220	235	260	285
	6.11E-03	205	225	245	260
	7.64E-03	190	210	225	240
	9.16E-03	175	190	210	225
2Methoxy ethanol	1.26E-03	310	340	370	390
	2.52E-03	300	320	350	375
	3.78E-03	285	310	325	345
	5.04E-03	265	285	300	325
	6.30E-03	250	265	290	310
	7.56E-03	225	250	270	290
Glycine	2.14E-03	290	330	360	395
	4.28E-03	275	295	330	360
	6.44E-03	250	270	300	325
	8.56E-03	235	255	280	300

Table 1 (continued)

	1.07E-02	215	240	265	290
	1.28E-02	200	220	240	265
Acetonitrile	1.90E-03	336	355	385	410
	3.80E-03	325	330	355	390
	5.70E-03	310	325	340	365
	7.60E-03	295	310	330	350
	9.50E-03	275	300	320	345
	1.14E-02	255	280	300	315

### Effect of Electrode Height on the Limiting Current

Fig. 4 show the effect of the electrode height on the limiting current in case of Cu-St. The limiting current density decreases with increase in height. In electrodeposition and generally for the cathodic deposition of metals, the direction of flow of the hydrodynamic boundary layer is upwards, the thickness of the hydrodynamic boundary layer and the diffusion layer increases in the upward direction, *i.e.*, the resistance to mass transfer increases in the upward direction, accordingly, the local limiting density increases in the upward direction of the cathode. The average limiting current density decreases with the increase in the height according to the equation.<sup>24</sup>

$$I_l = C/h^{0.31\pm} 0.01 \quad (2)$$

where C is constant, h is the height and  $I_l$  is the limiting current density.

### Effect of Organic Substance on the Limiting Current under Natural Convection Flow

The % Inhibition can be calculated using the equation:

$$\% \text{ Inhibition} = (I - I_l / I) \times 100 \quad (3)$$

where I and  $I_l$  are electrodeposition limiting current values without and with inhibitor respectively, Fig. (5) show that the addition of organic compounds reduces the limiting current by amounts ranging from 2.9 % to 48.5 % (Cu-St cell) . Under natural convection mass is transferred outside the diffusion layer by natural convection which arises from the density difference between the interface solution

and the bulk solution while mass is transferred inside the diffusion layer by diffusion only by virtue of the existence of concentration gradient across the diffusion layer. In view of the above mechanism, the adverse effect of organic compounds on the limiting current can explain as follows: Organic compound adsorbed on the cathode surface increases the interfacial viscosity,  $\eta$  of the solution with a consequent decrease in diffusivity, D of  $\text{Cu}^{++}$  according to the Stokes-Einstein equation (4).<sup>26</sup>

$$D\eta / T = \text{constant} \quad (4)$$

Also, we show in Fig. 5, that the %Inhibition for all of the organic compounds slightly decreases with increasing temperature from 298 K to 313 K this may be explained by desorption of adsorbed inhibitor on the copper surface.<sup>26</sup>

### Adsorption isotherm

Two main types of interaction can describe the adsorption of organic compounds, namely: physical (electrostatic) adsorption and chemical adsorption (chemisorption) on the metal surface. These are dependent on the electronic structure of the metal, the nature of the electrolyte and the chemical structure of the inhibitor.<sup>27-30</sup> Mostly, organic compounds containing N, O or S groups or organic compounds having  $\pi$  bonds in their structures are found to be effective inhibitors in acid media. Also the presence of functional groups, such as =NH, -N=N-, -CHO, R-OH, C=C, etc., in the inhibitor molecule and also the steric factors, aromaticity, electron density of the donor atoms are found to influence the adsorption of the inhibitor molecules over the electrodepositing metal surface.<sup>31-34</sup>

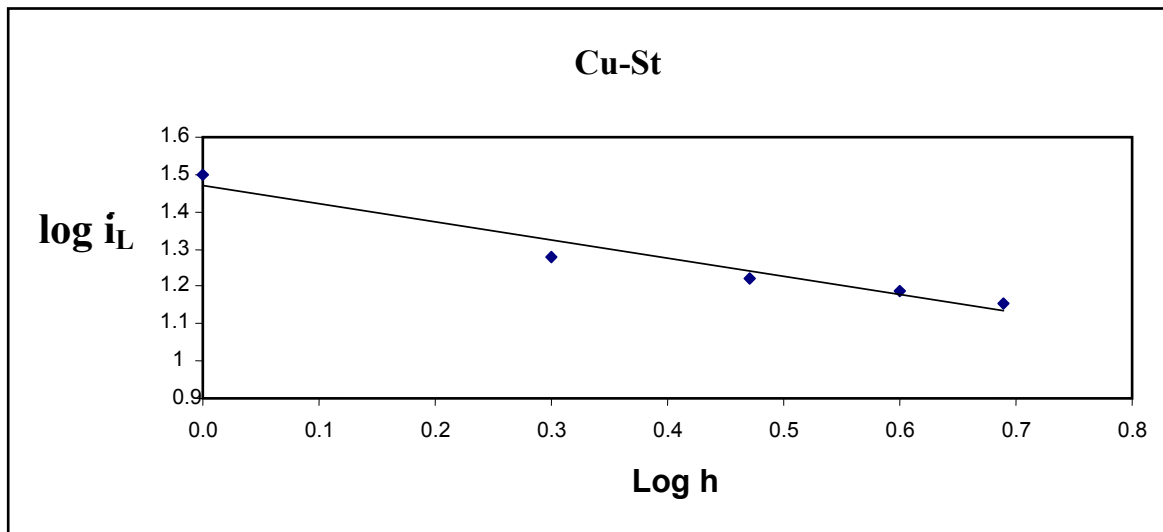
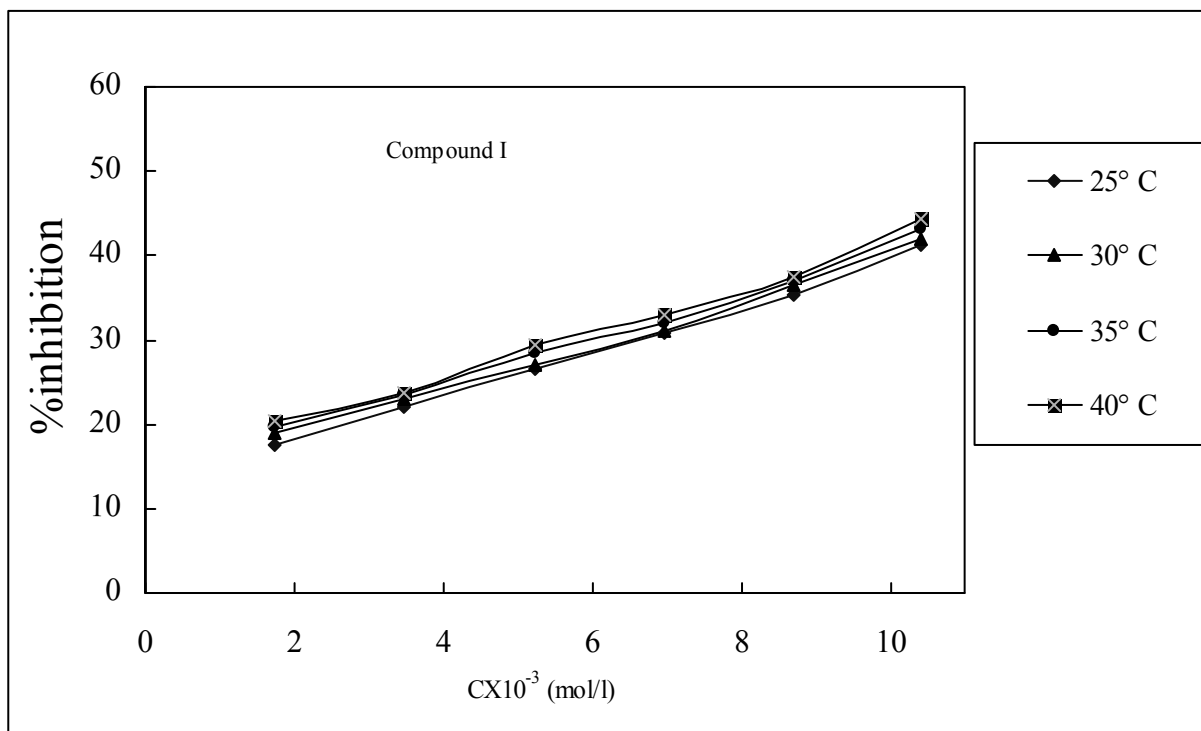
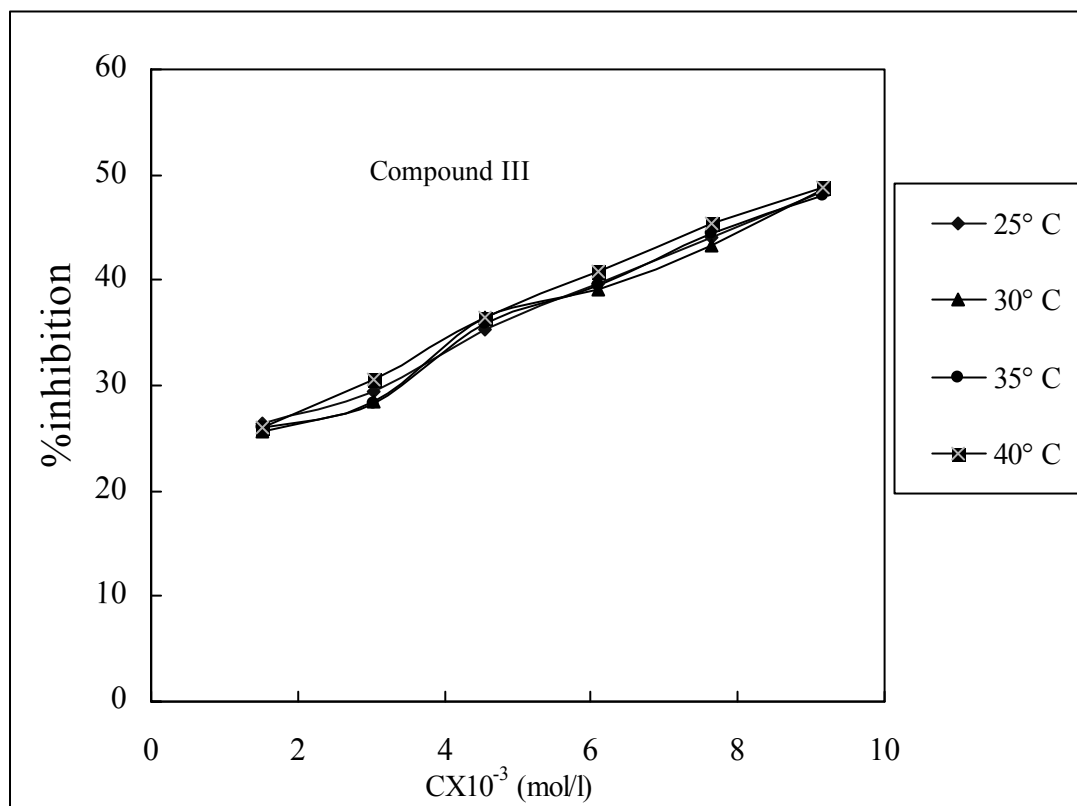
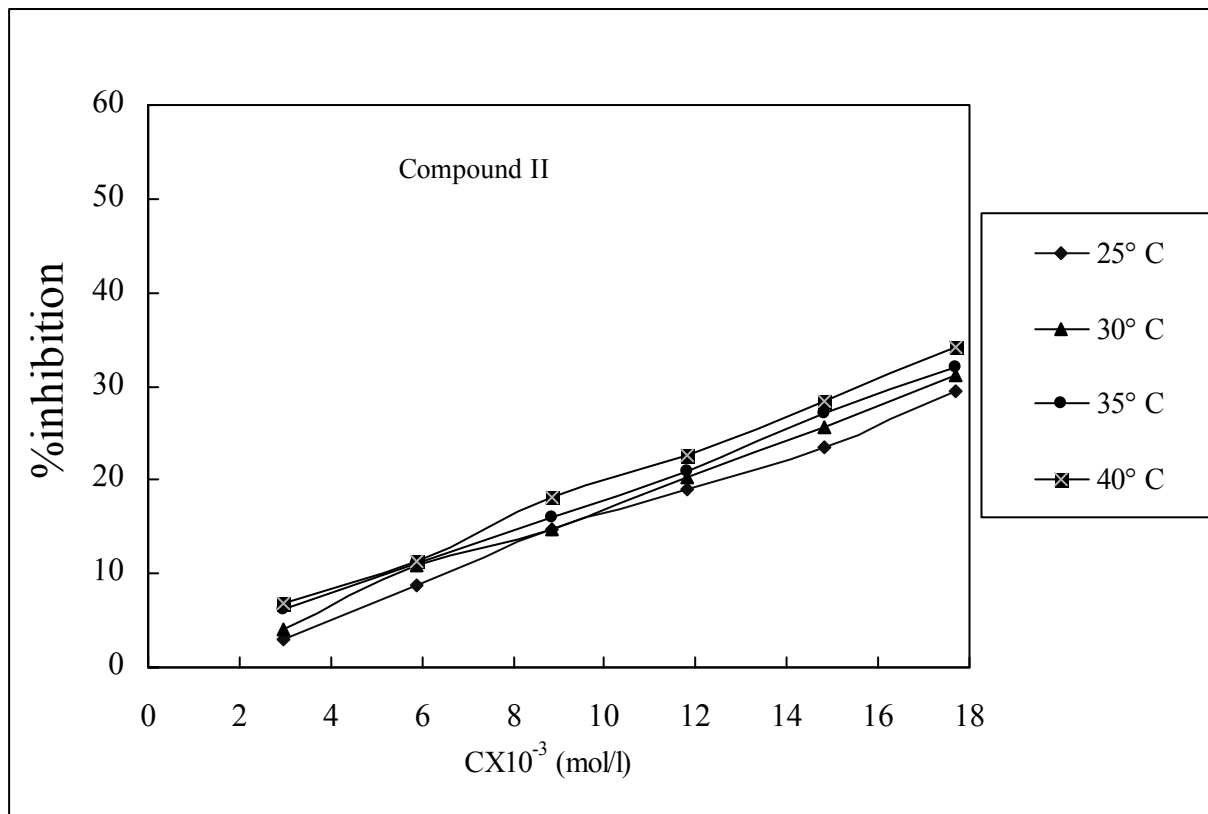
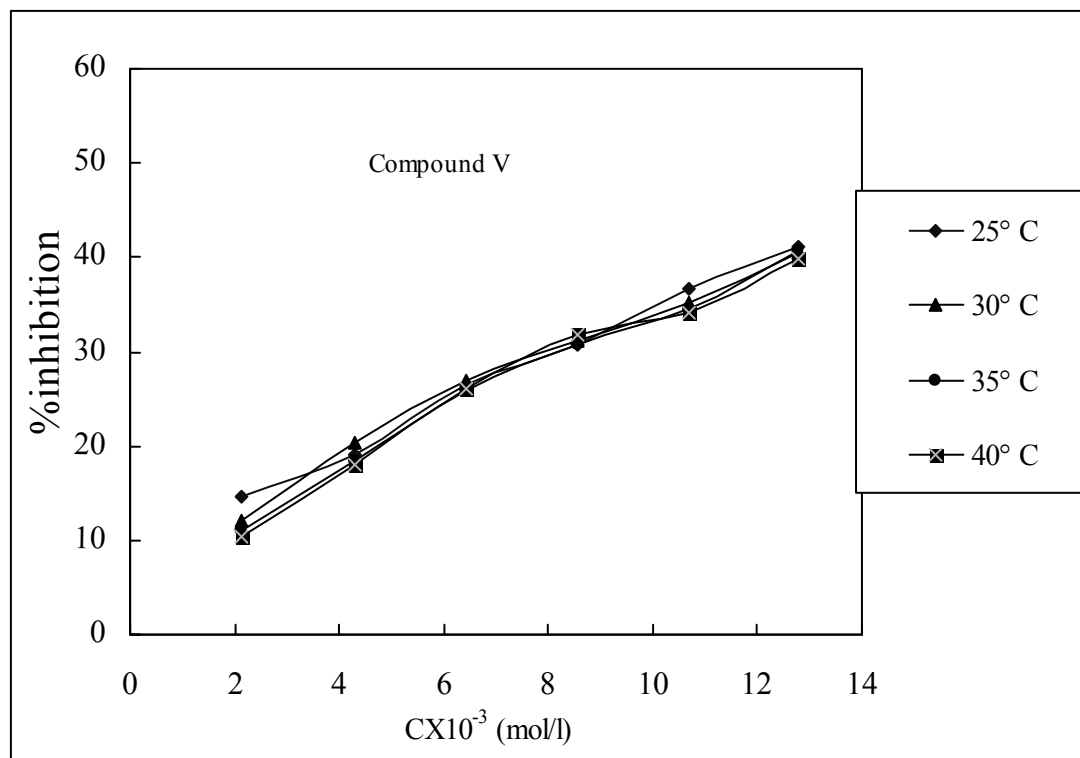
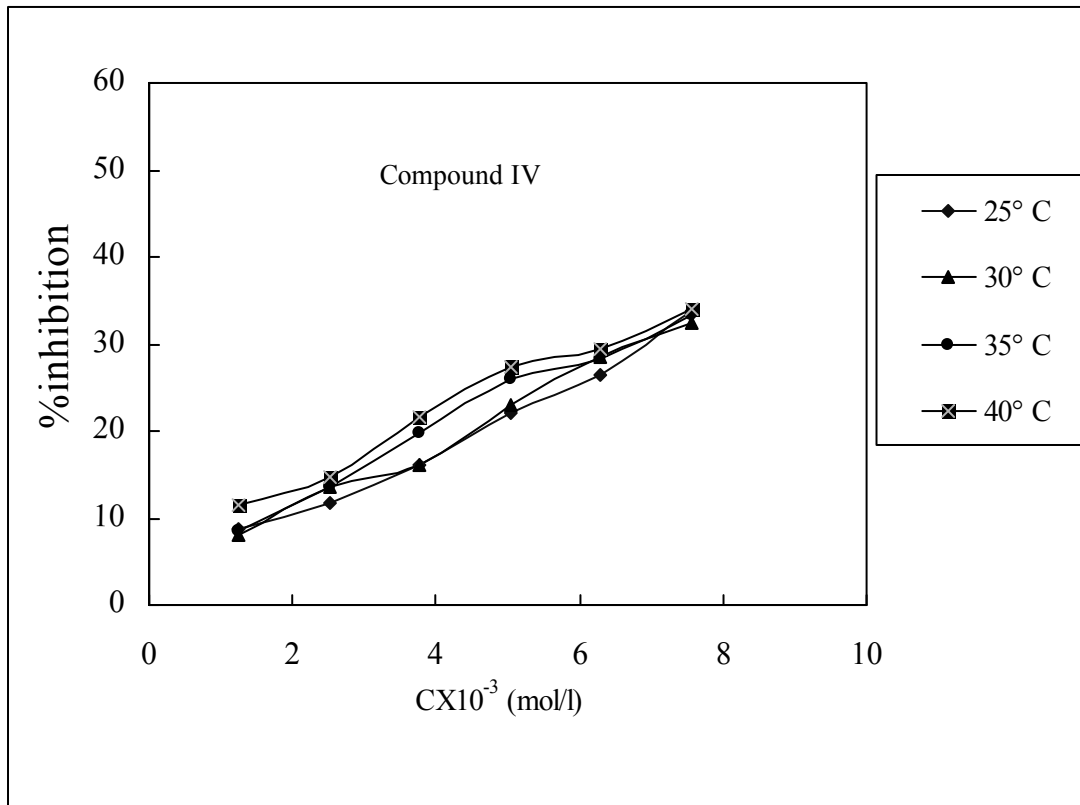


Fig. 4 – The relation between  $\log i_L$  &  $\log h$  in case of blank Cu-St at 298K.







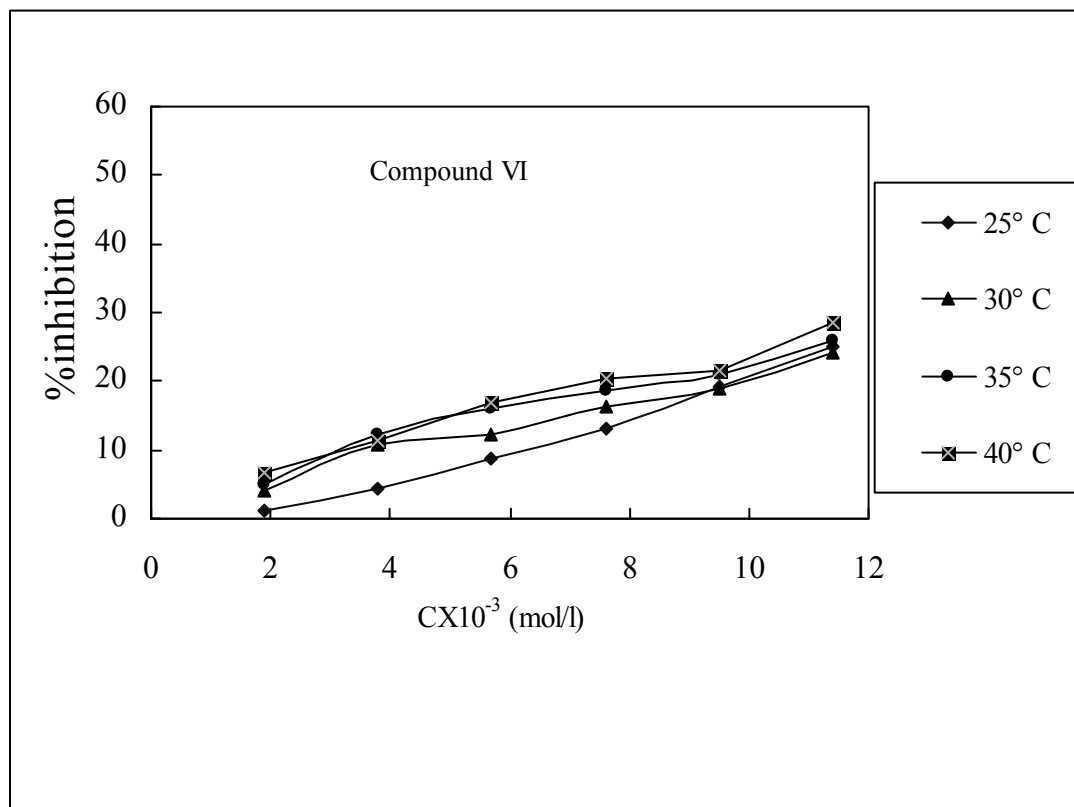
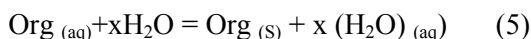


Fig. 5 – The effect of concentration of organic additives on the % inhibition of limiting current at different temperature for Cu-St cell.

The adsorption of the inhibitor molecules from aqueous solutions can be regarded as quasi-substitution process<sup>35</sup> between the organic compound in the aqueous phase, ( $\text{org}_{(aq)}$ ) and water molecules at the electrode surface, ( $\text{H}_2\text{O}_{(s)}$ )



where  $x$  (the size ratio) is the number of water molecules displaced by one molecule of organic inhibitor. Adsorption isotherms are very important for determining the mechanism of organo-electrochemical reactions. The most frequently used isotherms are those of Frumkin, Temkin, Florry-Huggins, Langmiur and Kinetic Isotherm.<sup>27-29</sup>

All these isotherms are of the general form:

$$f(\theta, x) \exp(-a\theta) = K C \quad (6)$$

where  $f(\theta, x)$  is the configuration factor depends essentially on the physical model and assumptions underlying the derivation of the isotherm.<sup>36</sup> The mechanism of inhibition of electrodeposition is generally believed to be due to the formation and maintenance of a protective film on the metal surface.<sup>37</sup> The primary step in the action of

thiosemicarbazide derivatives in acid solution is generally agreed to be adsorbed onto the copper surface. This involves the assumption that the electrodeposition reaction are prevented from occurring over the area (or the active sites) of the copper surface covered by adsorbed inhibitors species, whereas the electrodeposition reaction occurred normally in the inhibitor free area,<sup>38,39</sup> Accordingly, the fraction of the surface covered with inhibitor species ( $\theta$ ) can be followed as a function of inhibitor concentration and solution temperature. The part of the surface covered by inhibitor lead to decrease of limiting current. When fraction of the surface covered is determined as a function of the concentration at constant temperature, adsorption isotherm could be evaluated at equilibrium conditions. The values of fractional surface coverage ( $\theta$ ) at different concentrations of organic additives and at constant temperature have been used to explain the best isotherm to determine the adsorption process can be determined from.<sup>37-38</sup>

$$\theta = I - I_1 / I \quad (7)$$

Inhibitor adsorption characteristics can be estimated by using the Langmiur isotherm, which

is based on the assumption that all adsorption sites are equivalent and that molecule binding occurs independently from nearby sites being occupied or not given as:<sup>26-30</sup>

$$C/\theta = 1/K + C \quad (8)$$

where C is the concentration of organic additives (Inhibitor),  $\theta$  is fractional surface coverage and K is the adsorption equilibrium constant. Organic molecules having polar atoms or groups which are adsorbed on the metal surface may interact by mutual repulsion or attraction and this may be advocated as the reason for the departure of the slope values from unity.<sup>40,41</sup>

The characteristic of the Temkin adsorption isotherm<sup>29</sup> given by:

$$\text{Exp}(-2a\theta) = KC \quad (9)$$

where "a" is the lateral interaction parameter describing the molecular interaction in the adsorption layer and the heterogeneity of the metal surface. Linear plots obtained indicating that the experimental results of all additive studies obey the Temkin adsorption isotherm. The adsorption parameter deduced from Temkin adsorption isotherm is presented in Table 3. The molecular interaction parameter "a" can have both positive and negative values. Positive values of "a" indicates attraction forces between adsorbed molecules, while negative values indicate repulsive forces between the adsorbed molecules. It is seen in Table 2 that the values of "a" in all cases are negative, indicating that repulsion exists in the adsorption layer. It is generally known that K denotes the strength between the adsorbate and adsorbent. Large values of K imply more efficient adsorption.<sup>29</sup> The equation of Florry – Huggins Isotherm

$$\log \theta / C = \log xK + x \log (1 - \theta) \quad (10)$$

where x is the number of active sites occupied by one inhibitor molecule or number of water molecules replaced by one molecule of the adsorbate. The value of  $x > 1$ , implied that one inhibitor molecule replace more than one water molecule.<sup>50</sup> The plots of  $\log \theta / C$  against  $\log (1 - \theta)$  are shown in Figures (6) for compound I, III, IV, V, VI in Cu-St cell. The kinetic -thermodynamic model is given by:

$$\log [\theta / (1 - \theta)] = \log K' + y \log C \quad (11)$$

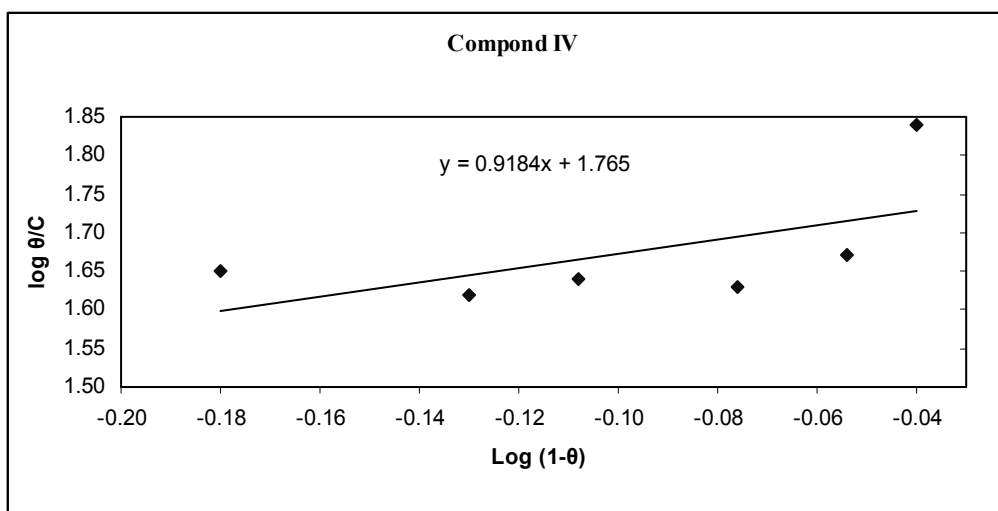
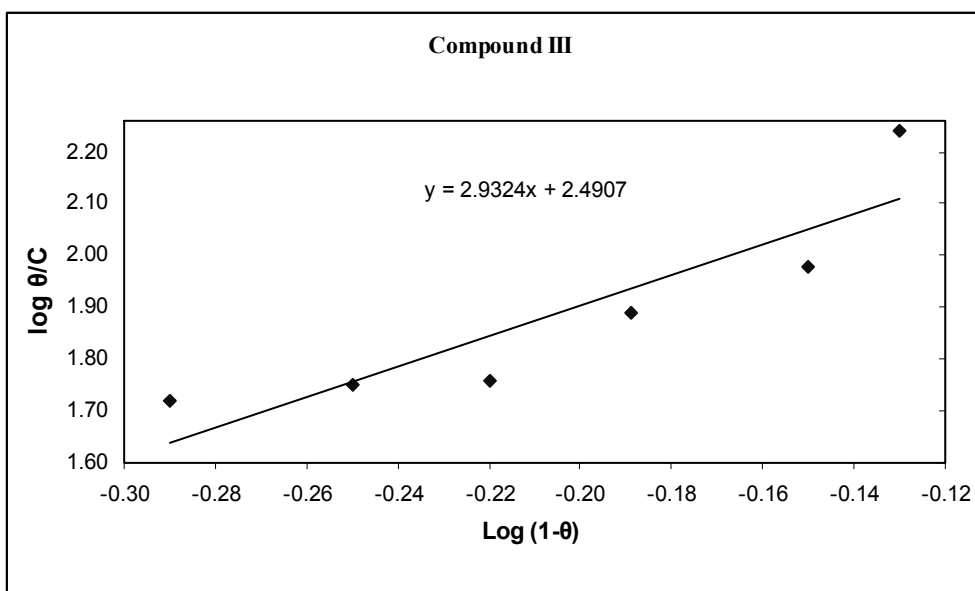
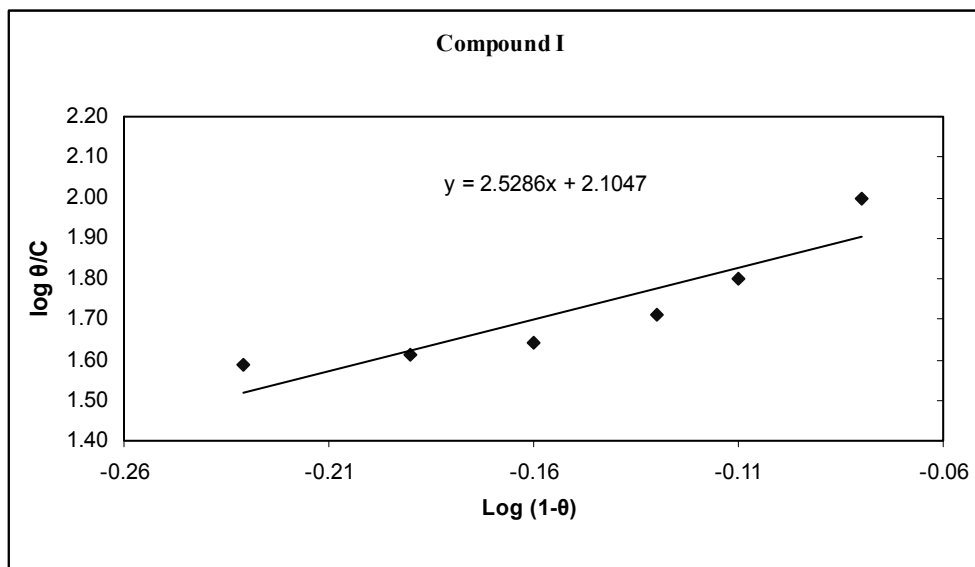
where y is the number of inhibitory molecules occupying one active site. The binding constant K is given by:<sup>50</sup>

$$K = K' (1/y) \quad (12)$$

If the slope y of the linear relation between  $\log \theta / (1 - \theta)$  vs.  $\log (C)$  for all organic compounds, is greater than unity implies the formation of multi-layers of the additive on the metal surface, while if less than unity, however, it means that the given additive molecule occupied more than one active site. Values of y and number of active sites  $1/y$  of the metal surface that occupied by one molecule of the organic additive under the present conditions have given in Table (2). Obviously, it was concluded from the values in Table (2) that the number of additive molecules, which occupy one active site, in some cases less than unity and in other cases greater than unity.<sup>41-45</sup> Also the efficiency of electrodeposition is an essential function of the magnitude of its binding constant K. Larger values of K mean better and strong interaction, whereas smaller values of K mean that the interaction between the additive molecules and metal surface is weaker.<sup>50-53</sup> The free energy of adsorption ( $\Delta G_{\text{ads}}$ ) at different concentrations of organic additives calculated from the equation:<sup>41</sup>

$$\Delta G_{\text{ads}} = -RT \ln (55.5 K) \quad (13)$$

The value 55.5: is the molar concentration of solvent (mol/l) which in our case is water. The values of ( $\Delta G_{\text{ads}}$ ) are given in Table (3) and the negative values in all cases means that spontaneous adsorption of inhibitor on the copper surface and strong interaction between the inhibitor molecules and metal surface. The most efficient inhibitor shows the most negative ( $\Delta G_{\text{ads}}$ ) value. This suggests that they strongly adsorbed on the metal surface. The ( $\Delta G_{\text{ads}}$ ) values are negative in Cu-St, so more positive than  $-40 \text{ kJmol}^{-1}$  indicating physical adsorption that means the adsorption of organic additives take place through electrostatic interaction between the inhibitor molecule and the metal surface. While ( $\Delta G_{\text{ads}}$ ) values about  $-40 \text{ kJmol}^{-1}$  or higher involve charge sharing or a transfer from the inhibitor molecules to the metal surface to form, a co-ordinate type of bond indicates chemical adsorption.<sup>45-49</sup> According to ( $\Delta G_{\text{ads}}$ ) values; all compounds follow the order of inhibition that is shown before St anode by using different organic compounds.



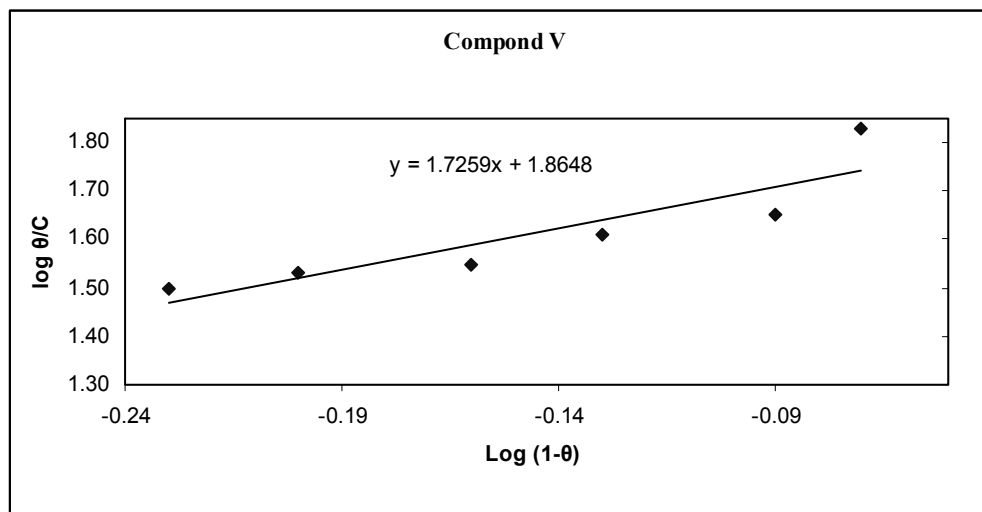


Fig. 6 – Florry – Huggins adsorption isotherm using Cu-St cell.

Table 2

Linear fitting parameters of thiosemicarbazide derivatives for (Cu-St) at 298 K

Organic Compounds	Models Parameters								
	Langmiur		Temkin		Flory-Huggins		Kinetic adsorption Isotherm		
	K	Slope	a	K	X	K	y	1/y	K
	Compound I	1.12	0.1754	-0.1297	2576.015	2.5286	50.3291	0.5779	1.73
Compound II			-0.1640	357.425			1.4284	0.7	94.732
Compound III	2.1589	0.1704	-0.1433	4348.08	2.9324	105.554	0.5388	1.856	19.818
Compound IV			-0.1544	1149.68			0.9269	1.078	42.258
Compound V	7.05E-01	0.1429	-0.1701	1047.1000	1.7259	42.441	0.7938	1.259	25.86
Compound VI			-0.1386	496.4640			1.7137	0.583	406.60

Table 3

Calculated values of free energy of adsorption  $\Delta G_{ads}$  (kJmol<sup>-1</sup>) for different organic compounds using different models for Cu-St

Organic compound		Cu-St cell		
		Temkin	Flory-Huggins	Kinetic adsorption
		$\Delta G_{ads}$	$\Delta G_{ads}$	$\Delta G_{ads}$
I	Compound	-29.4	-19.65	-16.56
II	Compound	-24.5		-21.22
III	Compound	-30.69	-21.49	-17.35
IV	Compound	-27.4		-19.22
V	Compound	-27.4	-19.23	-18
VI	Compound	32	-30.40	

### Effect of Temperatures and Thermodynamic Treatment of the reaction

The effect of temperatures on the electrodeposition rate of Cu-St cell in the absence and presence of all organic additives were studied by measuring the limiting current in the temperature ranges between (298-313 K) and illustrated in Table (1) and Figs.(7). It observed that the electrodeposition rate increases with temperature for all the studied systems and its extent more pronounced in the uninhibited system, indicating the physical adsorption of additives on the metal surface and desorption, aided by increasing the reaction temperature. Table (1) gives the variation of  $I_L$  with temperature at different concentration of organic compounds.<sup>50</sup> It can be seen that  $I_L$  increases for all organic compounds by desorption of adsorbed inhibitor from the copper surface.<sup>42</sup> The electrodeposition reaction can be regarded as an Arrhenius – type process. The activation energy for the studied systems calculated from the Arrhenius equation.<sup>43</sup>

$$\log I_L = \log A - E_a / 2.303 RT \quad (14)$$

where A is, a pre-exponential factor related to concentration, steric effects, metal surface

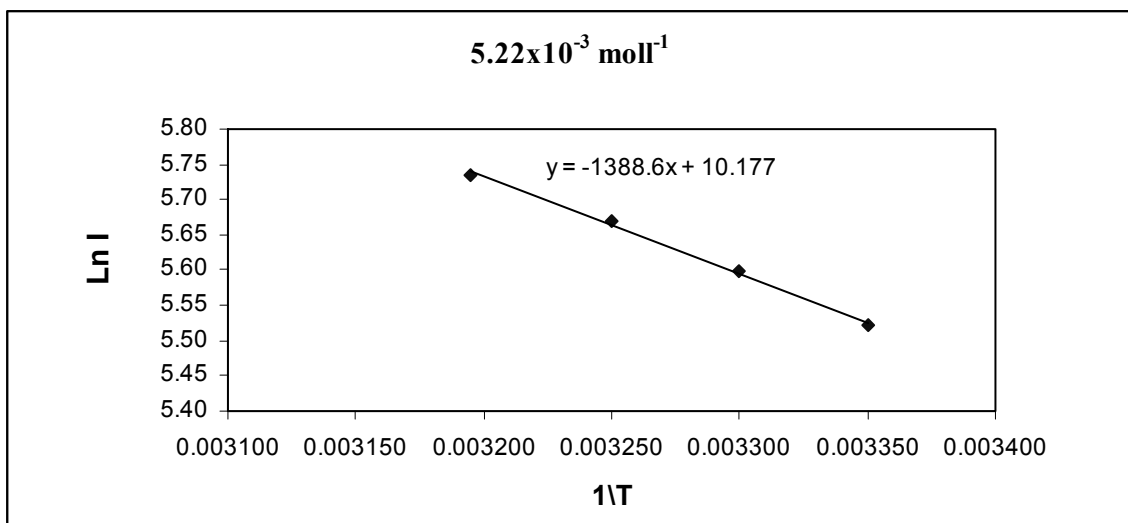
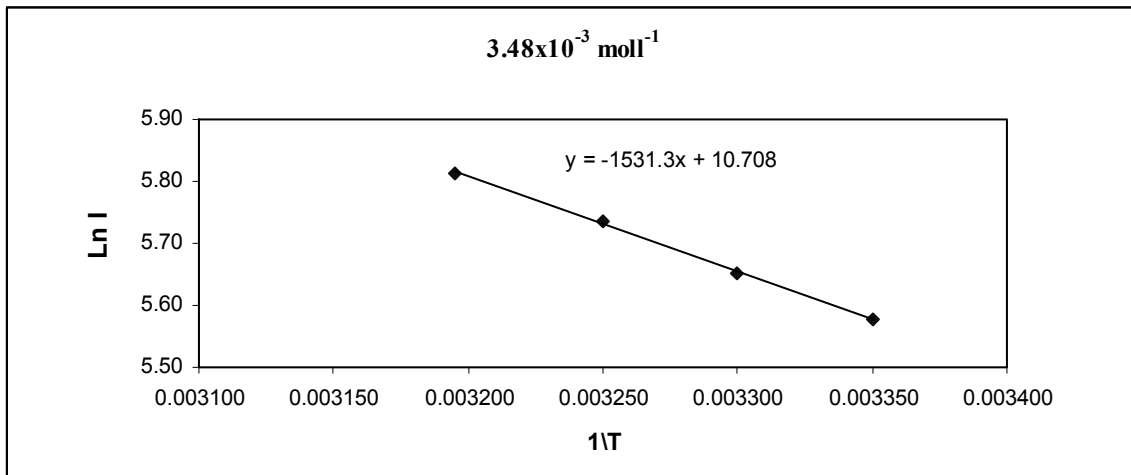
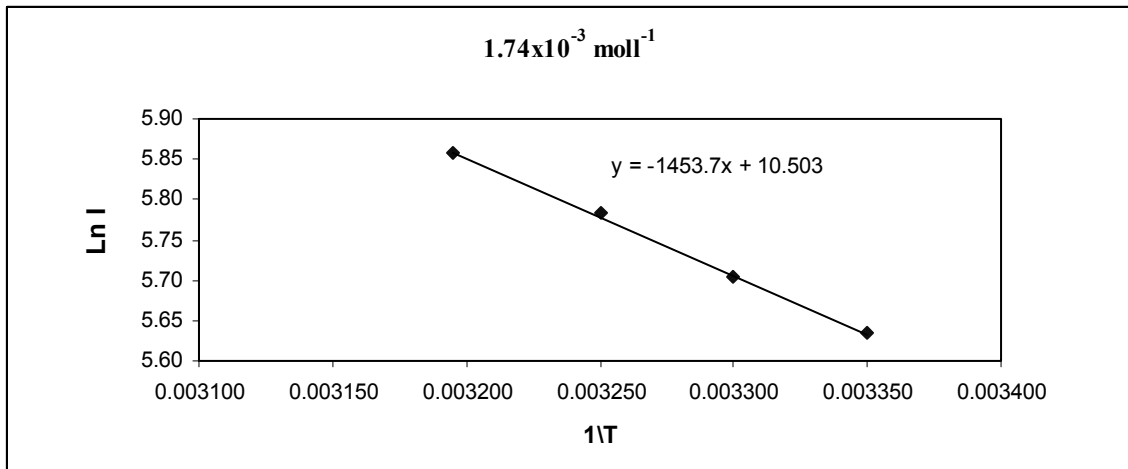
$$\log (I_L / T) = [(\log (R/hN) + (\Delta S^* / 2.303 R)] - \Delta H^* / 2.303 RT \quad (15)$$

where N is the Avogadro's number, h is the plank's constant. The change in the activation free energy  $\Delta G^*$ , of the electrodeposition, process calculated by applying the famous equation:

$$\Delta G^* = \Delta H^* - T\Delta S^* \quad (16)$$

characteristics, etc., R the molar gas constant and T absolute temperature. Values of  $E_a$  that have derived from the slopes of the Arrhenius plots are given in Table 5. It is an important thermodynamic parameters for determining the rate-controlling step. It is well known that when the rate-controlling step is the diffusion of aqueous species in the boundary layer  $E_a$  is generally  $\leq 28$  kJmol<sup>-1</sup>, while a value, usually  $> 43$  kJmol<sup>-1</sup> if adsorption of species on the reaction surface and subsequent chemical reaction take place.<sup>44</sup>

The results showed positive signs for  $E_a$ , reflecting the endothermic nature of electrodeposition process. It is obviously seen that the  $E_a$  values for inhibiting systems are higher than  $E_a$  for uninhibited system. This indicates that physical adsorption occurred in the first stage, which explains the nature of organic molecules – metal interaction. On the other hand, physical adsorption is related to lower values of  $E_a$  ( $< 43$  kJ.mol<sup>-1</sup>), also indicating that the diffusion processes are controlling the electrodeposition reaction.<sup>42-44</sup> Thermodynamic parameters ; the enthalpy of activation,  $\Delta H^*$ , entropy of activation,  $\Delta S^*$ , and the free energy of activation,  $\Delta G^*$ , are recorded in Table 4 and have been calculated from the transition state equation:



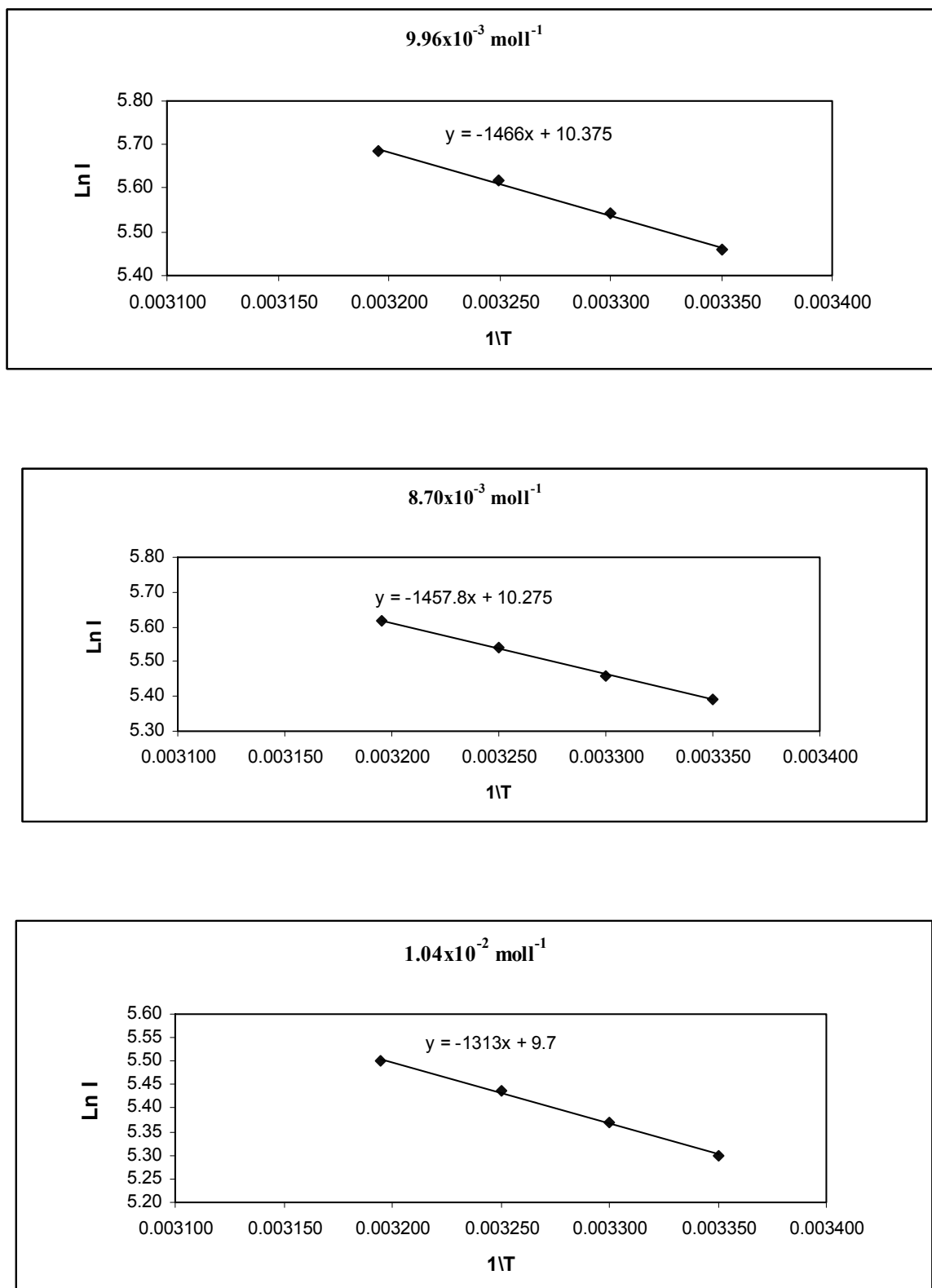


Fig. 7 – Relation between  $\ln I$  and  $1/T$  at different concentration of compound I for (Cu-St) cell.

Table 4

Activation energy and thermodynamic parameters for electrodeposition of copper in presence of different organic additives

Organic Compound	C (mol/L)	Cu-St			
		$E_a$	$\Delta H^*$	$\Delta S^*$	$\Delta G^*$
Compound I	Blank	14.04	11.57	-157.71	58.57
	1.74E-03	12.09	9.61	-165.89	59.04
	3.48E-03	12.73	10.25	-164.18	59.18
	5.22E-03	11.54	9.07	-168.60	59.31
	6.96E-03	12.19	9.71	-166.95	59.46
	8.70E-03	12.12	9.64	-167.78	59.39
	1.04E-02	10.92	8.44	-172.56	59.86
Compound II	Blank	14.04	11.57	-157.71	58.57
	2.95E-03	11.61	9.13	-166.11	58.63
	5.90E-03	12.54	10.07	-163.53	58.79
	8.85E-03	11.71	9.23	-166.80	58.93
	1.18E-02	11.57	9.09	-167.73	59.08
	1.48E-02	10.43	7.95	-172.07	59.23
	1.77E-02	10.35	7.87	-172.98	59.42
Compound III	Blank	14.04	11.57	-157.71	58.57
	1.53E-03	14.07	11.59	-160.11	59.30
	3.04E-03	13.02	10.54	-163.91	59.39
	4.56E-03	14.17	11.70	-160.93	59.66
	6.11E-03	12.81	10.33	-165.94	59.78
	7.64E-03	12.36	9.89	-168.05	59.97
	9.16E-03	13.79	11.31	-164.04	60.19
Compound IV	Blank	14.04	11.57	-157.71	58.57
	1.26E-03	12.47	9.99	-163.66	58.76
	2.52E-03	12.22	9.74	-164.84	58.87
	3.78E-03	9.99	7.51	-172.66	58.96
	5.04E-03	10.71	8.23	-170.93	59.17
	6.30E-03	12.35	9.87	-165.98	59.33
	7.56E-03	13.46	10.98	-162.97	59.55
Compound V	Blank	14.04	11.57	-157.71	58.57
	2.14E-03	16.33	13.86	-151.23	59.92
	4.28E-03	14.89	12.41	156.66	59.10
	6.44E-03	14.36	11.89	159.17	59.32
	8.56E-03	13.29	10.81	163.26	59.47
	1.07E-02	16.05	13.57	154.72	59.63
	1.28E-02	15.01	12.53	158.86	59.87
Compound VI	Blank	14.04	11.57	-157.71	58.57
	1.90E-03	10.93	8.46	-168.22	58.59
	3.80E-03	10.09	7.61	-171.49	58.72
	5.70E-03	8.63	6.16	-176.61	58.79
	7.60E-03	9.29	6.81	-174.80	58.91
	9.50E-03	12.03	9.55	-166.16	59.07
	1.14E-02	11.29	8.81	-169.20	59.23

 $E_a$ ,  $\Delta H^*$  and  $\Delta G^*$  in kJ/mol,  $\Delta S^*$  in J/mol.K

The results showed positive signs for  $E_a$ , reflecting the endothermic nature of electrodeposition process. It is obviously seen that the  $E_a$  values for inhibiting systems are higher than  $E_a$  for uninhibited system. This indicates that physical adsorption occurred in the first stage, which explains the nature of organic molecules – metal interaction. On the other hand, physical

adsorption is related to lower values of  $E_a$  ( $< 43 \text{ kJ.mol}^{-1}$ ), also indicating that the diffusion processes are controlling the electrodeposition reaction.<sup>42-44</sup> Thermodynamic parameters; the enthalpy of activation,  $\Delta H^*$ , entropy of activation,  $\Delta S^*$ , and the free energy of activation,  $\Delta G^*$ , are recorded in Table 4 and have been calculated from the transition state equation:

$$\log (I_L / T) = [(\log (R/hN) + (\Delta S^* / 2.303 R))] - \Delta H^* / 2.303 RT \quad (15)$$

where  $N$  is the Avogadro's number,  $h$  is the plank's constant. The change in the activation free energy  $\Delta G^*$ , of the electrodeposition, process calculated by applying the famous equation:

$$\Delta G^* = \Delta H^* - T\Delta S^* \quad (16)$$

The results show positive sign for  $\Delta H^*$ , reflecting the endothermic nature of the adsorption process. The negative values of  $\Delta S^*$  pointed to a greater order produced during the process of activation. This can be achieved by the formation of an activated complex represents association or fixation with consequent loss in the degree of freedom of the system during the process.  $\Delta G^*$  values show limited increase with a rise in the concentration of organic additives *i.e.*:  $\Delta G^*$  values of the inhibited systems were more positive than that for the uninhibited systems revealing that in the cores of inhibitor addition the activated electrodeposition complex becomes less stable as compared to its absence.<sup>51,52</sup>

### The isokinetic relationship

Variation in the rate within a reaction series may be caused by changes in either, or both, the enthalpy or the entropy of activation. The correlation of  $\Delta H^*$  with  $\Delta S^*$  is a linear relationship may be stated algebraically;

$$\Delta H^* = \beta \Delta S^* + \text{constant} \quad (17)$$

$$\delta \Delta H^* = \beta \delta \Delta S^* \quad (18)$$

The operator,  $\delta$ , concerns the difference between any two reactions in the series. Substituting from (18) into the familiar relationship:

$$\delta \Delta H^* = \delta \Delta G^* + T \delta \Delta S^* \quad (19)$$

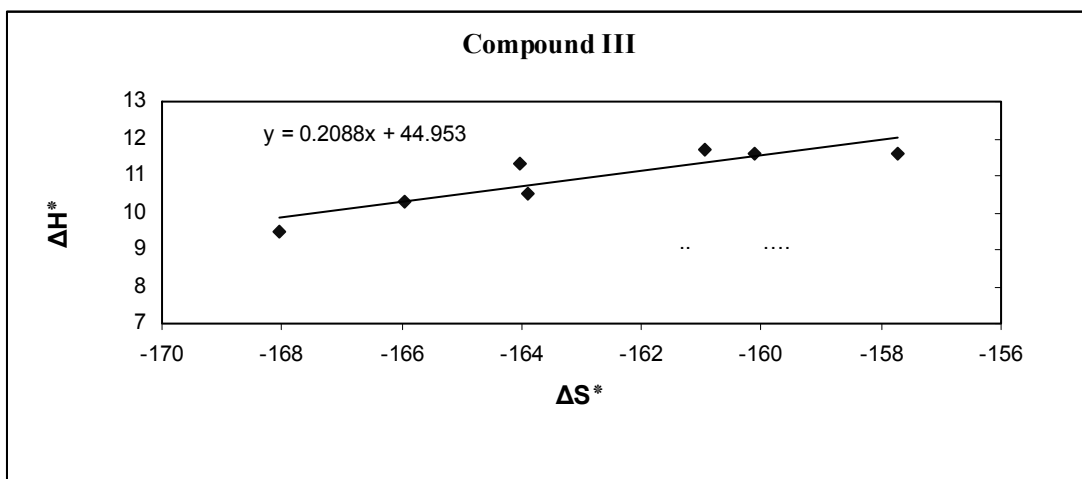
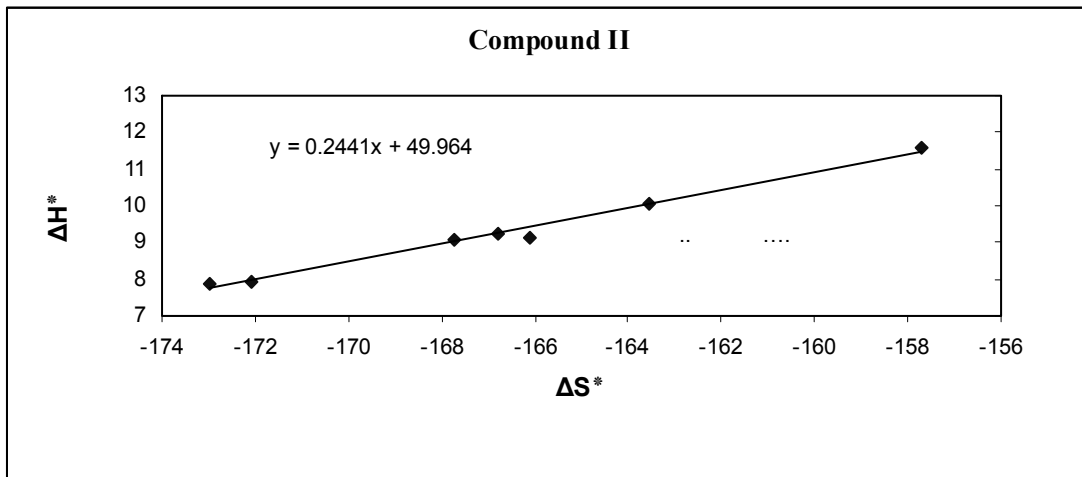
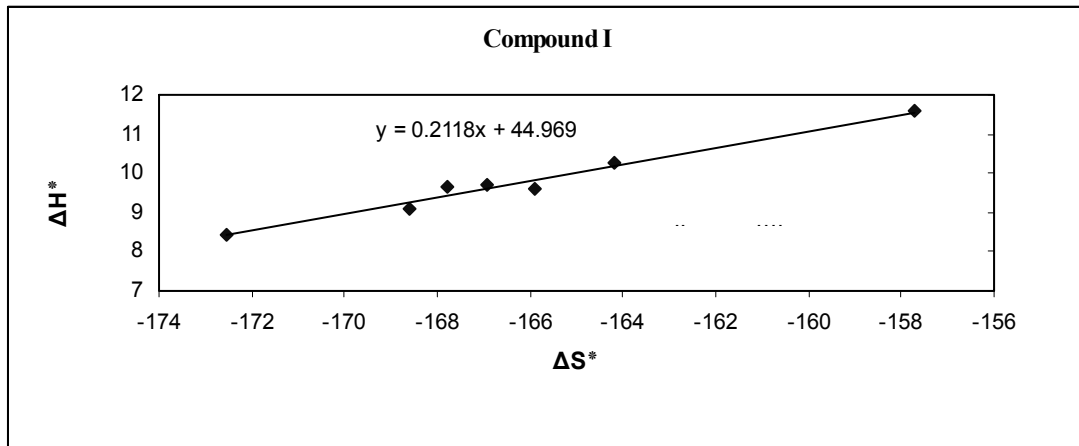
We obtain

$$\beta \delta \Delta S^* = \delta \Delta G^* + T \delta \Delta S^* \quad (20)$$

It follows that when  $\delta \Delta G^*$  equal zero,  $\beta$  equals  $T$ . In other words, the slope in a linear plot of  $\Delta H^*$  versus  $\Delta S^*$  is the temperature at which all the reactions that conform to the line occur at the same rate.  $\beta$  is therefore known as the isokinetic temperature. Fig. 8 show the plot of  $\Delta H^*$  versus  $\Delta S^*$  in presence of organic additives, the isokinetic temperature  $\beta$  were estimated as 211.8 & ,244.1 & .208.8 & ,276.2 & 262.5 & , and 287.9 K for for compounds, I, II, III, IV, V and VI , respectively in case of Cu-St cell . Which smaller than 298 K indicates that the rate of the reaction is entropy control.

The rotating cylinder electrode (RCE) configuration is one of the most used electrochemical configurations for electrochemical processes study. It is often used by the turbulent flow regime for industrial application such as intensive corrosion or electrodeposition processes. The effect of the speed of rotation on the electrodeposition rate can also be used to determine whether the electrodeposition process is diffusion or chemically controlled process. If the limiting current density increase by increasing the speed of rotation, then the reaction is diffusion controlled. However, if the limiting current is independent of the rotation, so the reaction is likely to be chemically controlled. The angular velocity,  $\omega$ , is related to the speed of rotation by:

$$\omega = 2\pi \text{ rpm} / 60 \quad (21)$$



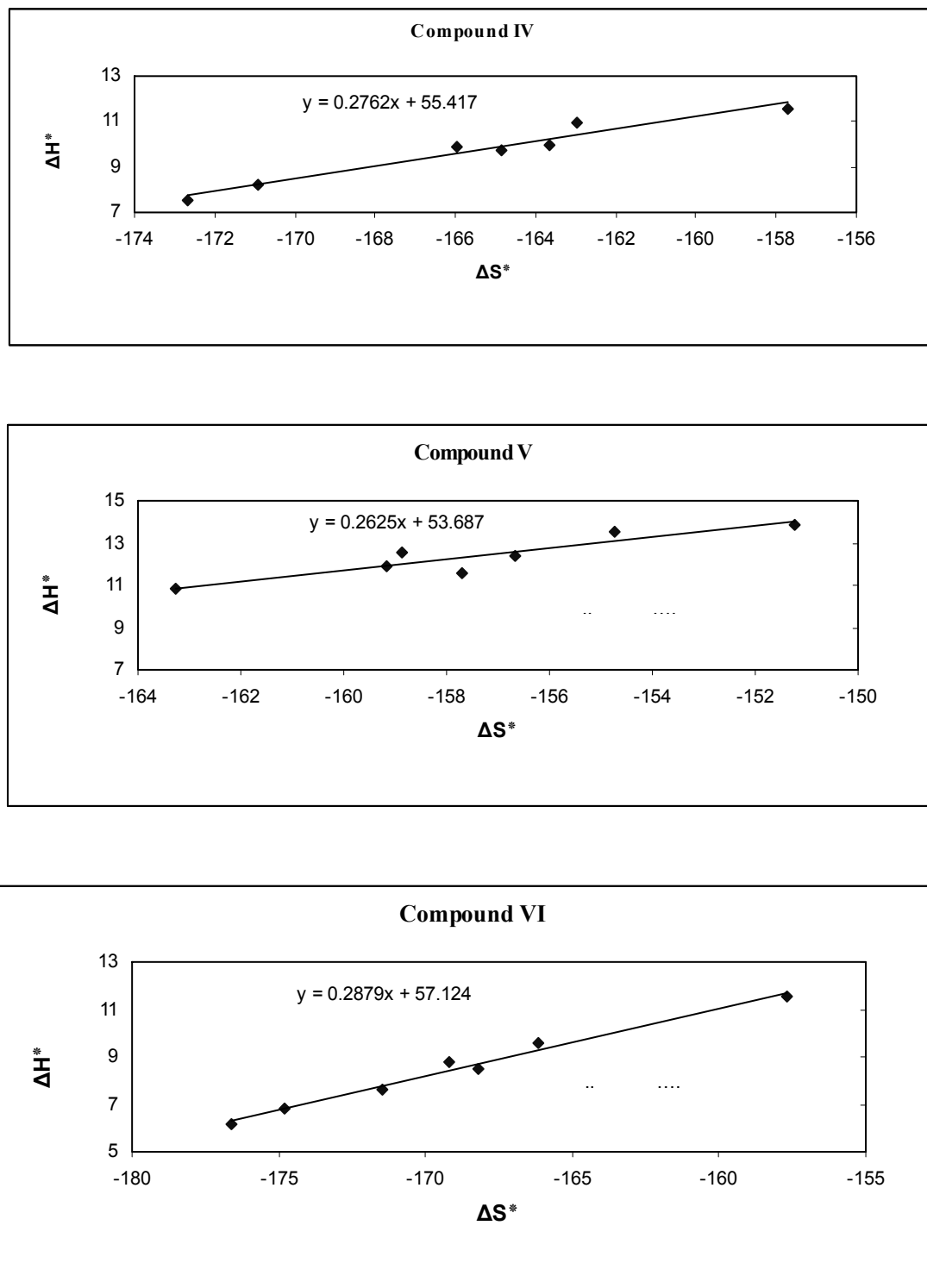


Fig. 8 –  $\Delta H^*$  vs.  $\Delta S^*$  of Cu-St for all organic compounds.

Figs. 4 show the relation between the limiting current density and the angular velocity to a power 0.7 for RCE at 298 K for the different organic additives used. Straight lines were obtained and the limiting current density

increases by increasing rotation, which indicates that the electrodeposition process of copper is diffusion controlled reaction. The diffusion coefficient of  $\text{Cu}^{++}$  ions,  $D$ , in different solutions was determined from the values of limiting

current density, as shown in Table (1), using Eisenberg equation<sup>45</sup>

$$i_L = k n F C_b d^{-0.3} \nu^{-0.344} D^{0.644} U^x \quad (22)$$

where,  $n$  is the number of exchanged electrons,  $F$  is faraday's constant  $nF$  is called "faradic equivalence",  $C_b$  is the bulk concentration ( $\text{mol cm}^{-3}$ ),  $U$  is the peripheral velocity  $= \omega r$  in  $\text{cm rad.s}^{-1}$  (where,  $\omega$  is the angular velocity and in  $\text{rad.s}^{-1}$ , and  $r$  is the radial distance in  $\text{cm}$ ) or  $U = 2\pi \omega r$  in  $\text{cm s}^{-1}$ ,  $d$  is the characteristic length for the rotating cylinder = the diameter of the cylinder in  $\text{cm}$ ,  $D$  is the diffusion coefficient for the metal ions ( $\text{Cu}^{2+}$  ions in our case)  $\text{cm}^2 \text{s}^{-1}$ ,  $\nu$  is the kinematics viscosity in Stoke ( $\nu = \eta/\rho$ ). The diffusion coefficient;  $D$ , of  $\text{Cu}^{2+}$  ions in solutions containing organic solvents decreases due to the increase in the interfacial viscosity;  $\eta$  in accordance<sup>46</sup> with the Stokes-Einstein equation 23

$$\frac{\eta D}{T} = \text{constant} \quad (23)$$

where:  $\eta$  is the viscosity of solution ( $\text{g.cm}^{-1}.\text{s}^{-1}$ ),  $D$  is the diffusion coefficient of copper ions ( $\text{cm}^2 \text{S}^{-1}$ ) and  $T$  is the absolute temperature ( $^\circ\text{K}$ ). The present results agree with the polarographic studies conducted in solution containing surfactants and also solution containing organic solvent, where it was found that the diffusion current decreases in the presence of surfactant and organic solvent.<sup>47</sup>

### Data Correlation

The mass transport to an inner rotating cylinder electrode in the turbulent flow system may be described by empirical dimensions

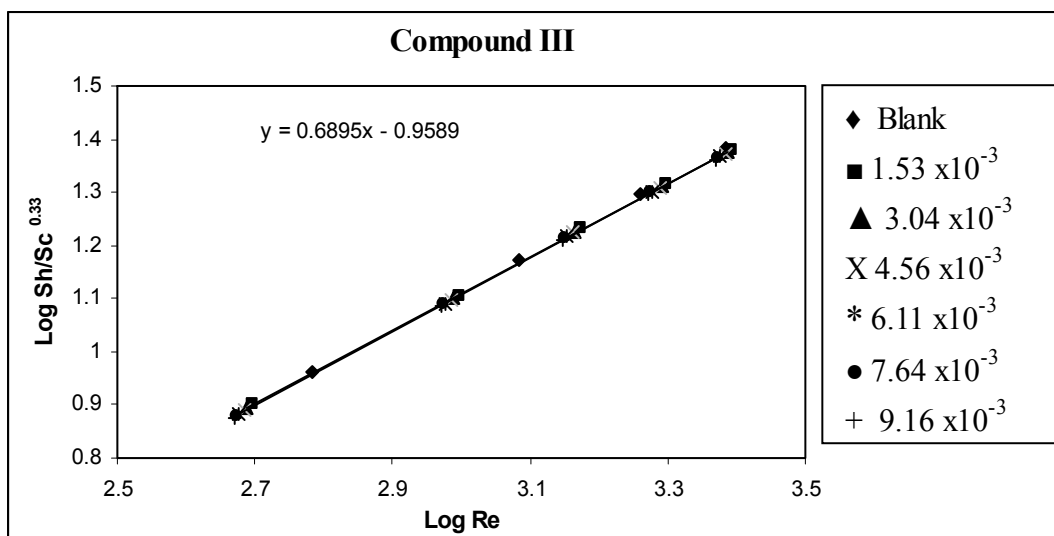
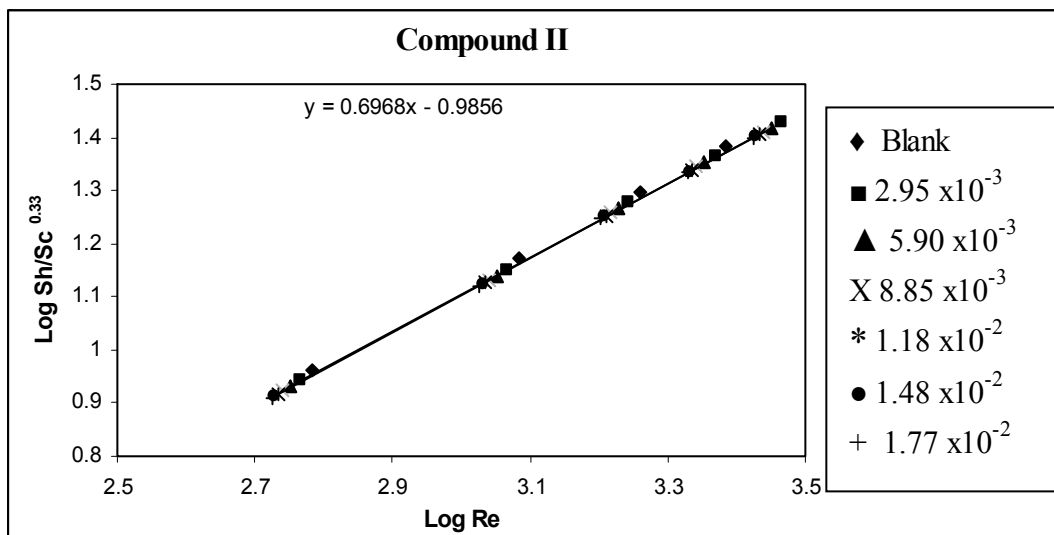
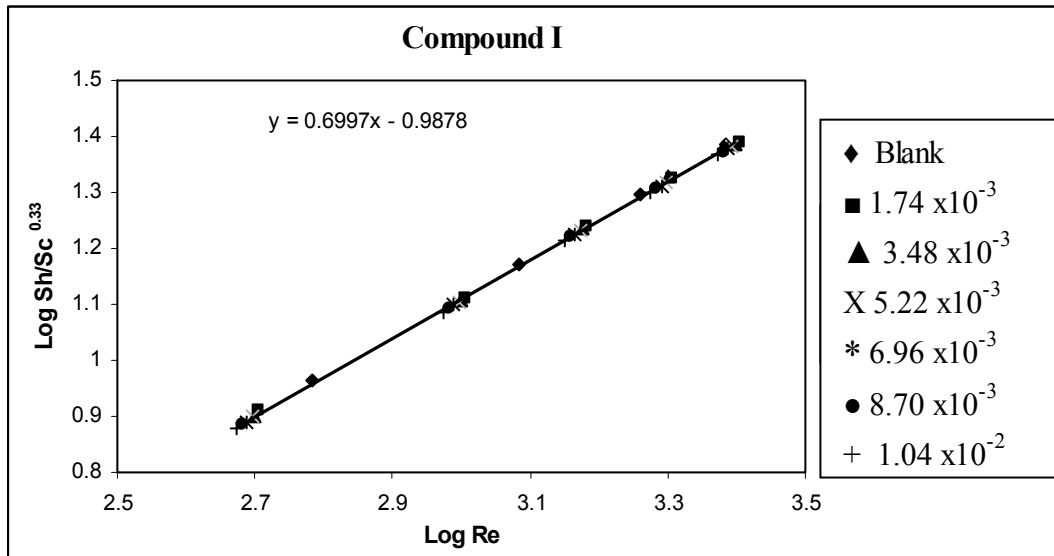
$$\text{Sh} = a \text{Sc}^c \text{Re}^b \quad (24)$$

where  $\text{Sh}$ ,  $\text{Re}$  and  $\text{Sc}$  are the Sherwood ( $\text{Sh} = \text{KL}/D$ ),  $k$  is mass transfer coefficient,  $\text{cm s}^{-1}$  ( $K = i_L/zFC$  ( $\text{Cu}^{2+}$ ) where  $C$  ( $\text{Cu}^{2+}$ ) is saturation solubility of copper sulphate,  $Z$  is the valance,  $F$  is Faraday's constant in  $\text{A s mol}^{-1}$ ),  $L$  is length of cylinder,  $\text{cm}$  and  $D$  is diffusion coefficient,  $\text{cm}^2 \text{s}^{-1}$ , Reynolds ( $\text{Re} = dU/\nu$ ),  $\nu$  is kinematic viscosity,  $\text{cm}^2 \text{s}^{-1}$  and  $U$  is rotation velocity  $= \omega r$ ,  $\text{cm s}^{-1}$ ,  $d$ : diameter of the cylinder in  $\text{cm}$  and ( $\text{Sc} = \nu / D$ ) numbers, respectively and  $a$  and  $b$  are empirical constants,  $c = 0.33$  indicating forced convection regime.<sup>29</sup> By plotting  $\log \text{Sh} / (\text{Sc}^{0.33})$  against  $\log \text{Re}$ , a straight line was obtained, its slope gave the constant "b" while the intercept gives the constant "a". Figure 9 shows the mass transfer correlation for all parameters used in case of RCE. From this Figure 9, the data can be correlated by the following equations:

$$\text{Blank Sh} = 0.1046\text{Re}^{0.6987} \text{Sc}^{0.33}$$

In our present study a forced convection mechanism is obtained which agree very well with similar relationships reported before.<sup>48-50</sup>

1.	For acidic acid solutions	$\text{Sh} = 0.1028 \text{Re}^{0.699} \text{Sc}^{0.33}$
2.	For formamide solutions	$\text{Sh} = 0.1034 \text{Re}^{0.697} \text{Sc}^{0.33}$
3.	For ethylamine solutions	$\text{Sh} = 0.1099 \text{Re}^{0.689} \text{Sc}^{0.33}$
4.	For 2-Methoxy ethanol solutions	$\text{Sh} = 0.1045 \text{Re}^{0.696} \text{Sc}^{0.33}$
5.	For glycine solutions	$\text{Sh} = 0.1065 \text{Re}^{0.693} \text{Sc}^{0.33}$
6.	For acetonitrile solutions	$\text{Sh} = 0.1022\text{Re}^{0.698} \text{Sc}^{0.33}$



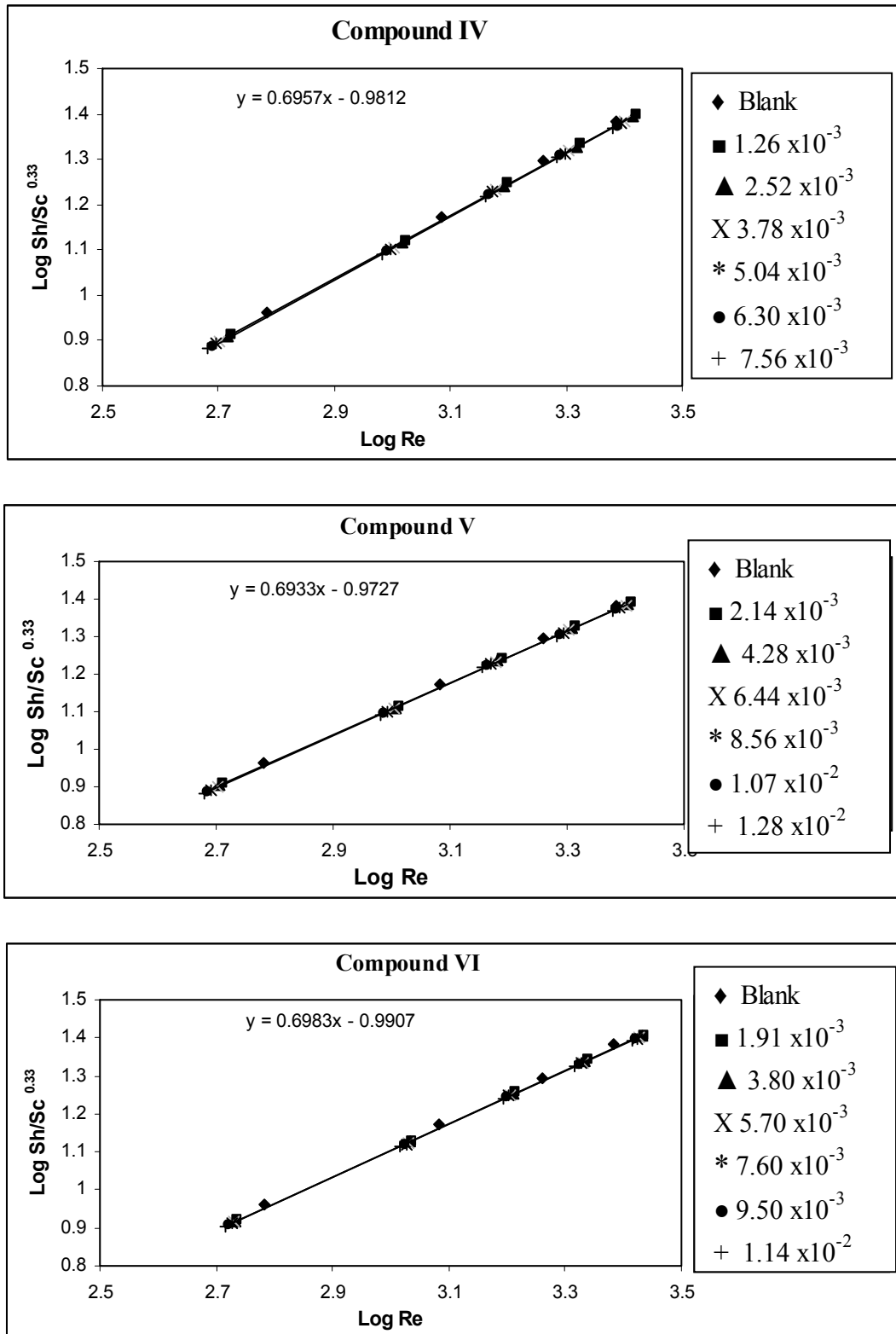


Fig. 9 – Overall correlation between  $\log \text{Sh/Sc}^{0.33}$  and  $\log \text{Re}$  for all organic compounds using cylinder electrode at 298 K.

## CONCLUSION

The values of inhibition efficiency of Cu deposition, increase with increasing inhibitor

concentrations and decrease slightly with temperature. Addition of organic acids did not change the diffusion controlled mechanism of Cu deposition to a charge transfer controlled mechanism.

The application of rotating cylinder electrodes (RCEs) to electrodeposition has progressed significantly over the last decade. New tools for theoretical and experimental investigations have been developed in academia and in industry, with some RCE devices being commercially developed. This paper reviews the continued application of RCEs to quantitative electrodeposition studies of single metals, alloys, and composite, multilayered, and nanostructured electrodeposits with a constant or controlled range of current densities along the RCE under turbulent flow conditions. Rotating cylinder electrode electrochemical reactors, enhanced mass transport, rotating cylinder Hull cell, and uniform and non-uniform current and potential distributions are considered. The applications of ultrasound, porous reticulated vitreous carbon cathodes, expanded metal/baffles, and jet flow around the RCE are also included. The effects of electrolyte flow and cathode current density on electrodeposition have been rationalized. Directions for future RCE studies are proposed.

## REFERENCES

- D. R. Gabe, G. D. Wilcox, J. Gonzalez-Garcia and F. C. Walsh, *J. Appl. Electrochem.*, **1998**, *28*, 759.
- J. Low, C. Ponce de León and F. C. Walsh, *Aust. J. Chem.*, **2005**, *58*, 246.
- J. L. Nava, E. Sosa, C. Ponce de León and M. T. Oropeza, *Chem. Eng. Sci.*, **2001**, *56*, 2695.
- G. Chen, *Sep. Purif. Technol.*, **2004**, *38*, 11.
- J. M. Grau and J. M. Bisang, *J. Chem. Technol. Biot.*, **2002**, *77*, 465.
- F. F. Rivera, I. González and J. L. Nava, *Environ. Technol.*, **2008**, *29*, 817.
- M. El BATOUTI and A. M. AHMED *Rev. Roum. Chim.*, **2015**, 1047.
- F. C. Walsh, *Pure Appl. Chem.*, **2001**, *73*, 1819.
- C. Madore, M. Matlosz and D. Landolt, *J. Appl. Electrochem.*, **1992**, *22*, 1155.
- N. Zech, E. J. Podlaha and D. Landolt, *J. Appl. Electrochem.*, **1998**, *28*, 1251.
- D. R. Gabe, *J. Appl. Electrochem.*, **1974**, *4*, 91.
- D. R. Gabe and F. C. Walsh, *J. Appl. Electrochem.*, **1984**, *14*, 555.
- J. M. Grau and J. M. Bisang, *J. Appl. Electrochem.*, **2006**, *36*, 759.
- A. H. Nahlé, G. W. Reade and F. C. Walsh, *J. Appl. Electrochem.*, **1995**, *25*, 450.
- F. F. Rivera and J. L. Nava, *Electrochim. Acta*, **2007**, *52*, 5868.
- T. Pérez, L. José and L. Nava, *Int. J. Electrochem. Sci.*, **2013**, *8*, 4690.
- J. Y. Hwang, K. S. Yang and K. Bremhorst, *J. Fluid Eng.*, **2007**, *129*, 40.
- J. Y. Hwang, K. S. Yang, D. H. Yoon and K. Bremhorst, *Int. J. Heat Fluid Fl.*, **2008**, *29*, 1268.
- E. P. Rivero, P. Granados, F. F. Rivera, M. Cruz and I. González, *Chem. Eng. Sci.*, **2010**, *65*, 3042.
- N. Ibl, P. Delahary and C.W. Tobias (Eds.), "Advances in Electrochemistry and Electrochemical Engineering", Interscience, New York, **1962**.
- N. Ibl, P. H. Javet and F. Stonel, *Electrochim. Acta*, **1972**, *17*, 733.
- F. Bruno and J. E. Dubis, *Electrochim. Acta*, **1972**, *17*, 1161.
- K. M. Ismail, *Electrochim. Acta*, **1972**, *52*, 7811.
- F. Lallemand, L. Rieq and M. Rieq, *Surf. Coat. Technol.*, **2004**, *179*, 314.
- L. Bonou, M. Eyraud, R. Denoyel and Y. Massiani, *Electrochim. Acta*, **2002**, *47*, 4139.
- E. Mc Cafferty, V. Pravdic and A. C. Zettlemoyer, *Trans. Faraday Soc.* **1999**, *66*, 237.
- N. M. Elmalah, F. A. Issa, A. M. Ahmed and L. F. Gado, *JDST*, **2010**, *31*, 1579.
- B. Ateya, B. El- Anadouli, and F. El- Nizamy, *Corros. Sci.* **1984**, *24*, 509.
- V. Chandradrase and K. Kannan, *Bull. Electrochem.*, **2004**, *20*, 471.
- E. E. Oguize, B. N. Okolue, C. E. Ogukwe, A. I. Onuchukwu, and C. Unaegbu, *Bull. Electrochem.*, **2004**, *20*, 421.
- R. Saratha, S.V. Priya and P. Thilagavathy, *E- J. Chem.* **2009**, *6*, 785.
- A. A. El-Awady, B. A. Abd El- Nabey, S. G. Aziz, *J. Electrochem. Soc.*, **1992**, *19*, 2149.
- P. J. Florry, *J. Chem. Phys.*, **1942**, *10*, 51.
- A. M. Abdel-Gaber, B. A. Abd El Nabey, I. M. Sidahmed, A. M. El-Zayady and M. Saadawy, *Corros. Sci.*, **2004**, *48*, 2765.
- N. Khalil, F. Mahgoub, B. A. Abd El- Nabey and A. Abd El- Aziz, *Cest*, **2003**, *38*, 205.
- K. M. Ismail, *Electrochemi. Acta*, **2007**, *52*, 7811.
- E.E. Oguzie, *Pigment Resin Techno.*, **2005**, *34*, 321.
- S. Bilgie and M. Shin, *Mater. Chem. Phys.*, **2001**, *70*, 290.
- H. M. Bhajwala and R. T. Vashi, *Bull. Electrochem.*, **2001**, *17*, 441.
- E. A. Noor, *Mater. Chem. Phys.*, **2009**, *114*, 533.
- M. Bouklah, N. Benchat, A. Aounit, B. Hammouti, M. Benkaddout, M. Lagreniee, H. Vezin and F. Bentiss, *Prog. Org. Coat.*, **2004**, *51*, 118.
- H. M. Soliman and H. H. Abd El – Rahman, *J. Braz. Chem. Soc.*, **2006**, *117*, 705.
- H. H. Abd El- Rahman and M. A. Darweesh, *Egypt J. Chem.*, **2006**, *49*, 19.
- C. Jeyaprabha, S. Sathiyarayanan, and G. Venkatachari, *Electrochim. Acta*, **2006**, *51*, 4080.
- M. Eisenberg, C. W. Tobias and C. R. Wilke, *J. Electrochem. Soc.*, **1954**, *101*, 306.
- G. M. El-Subruite and A. M. Ahmed, *Portugaliae Electrochim. Acta*, **2002**, *20*, 151.
- A. M. Ahmed and M. El Batouti and S. M. S. Khelil, *Portugaliae Electrochimica Acta*, **2015**, *33*, 105-11048. 48.
- M. El Batouti, S. Salaam, A. M. Ahmed and H. El Hamdy, *Asian J. Chem.*, **2016**, *28*, 965-970.
- H. M. Soliman and H. H. Abd El – Rahman, *J. Braz. Chem. Soc.*, **2006**, *117*, 705.
- H. Ashassi – Sorkhabr, B. Shabani and B. Aligholipour, *Appl. Surf. Sci.*, **2005**, *239*, 154.
- U. Mohete, K. M. Gadane and C. D. Lokhande, *Ind. J. Eng. Mat. Sci.*, **1995**, *2*, 93.
- J. R. Selman and C. W. Tobias, *Adv. Chem. Eng.*, **1987**, *10*, 211.
- M. El Batouti and A. M. Ahmed, *Asian J. Chem.*, **2016**, *28*, 479.